



# Thermal decomposition of the natural hydrotalcites carrboydite and hydrohonessite

Ray L. Frost<sup>a,\*</sup>, Matt L. Weier<sup>b</sup>, Meagan E. Clissold<sup>a</sup>,  
Peter A. Williams<sup>a</sup>, J. Theo Kloprogge<sup>b</sup>

<sup>a</sup> Centre for Industrial and Process Mineralogy, School of Science, Food and Horticulture,  
University of Western Sydney, Locked Bag 1797, Penrith South DC, NSW 1797, Australia

<sup>b</sup> Centre for Instrumental and Developmental Chemistry, Queensland University of Technology,  
G.P.O. Box 2434, Brisbane, Qld 4001, Australia

Received 19 February 2003; received in revised form 11 April 2003; accepted 12 April 2003

## Abstract

A combination of high-resolution thermogravimetric analysis (HRTGA) coupled to a gas evolution mass spectrometer combined with infrared emission spectroscopy has been used to study the thermal decomposition of two Australian hydrotalcites carrboydite ( $\text{Ni}_6\text{Al}_2(\text{SO}_4, \text{CO}_3)(\text{OH})_{16} \cdot 4\text{H}_2\text{O}$ ) and hydrohonessite ( $\text{Ni}_6\text{Fe}_2(\text{SO}_4, \text{CO}_3)(\text{OH})_{16} \cdot 7\text{H}_2\text{O}$ ). High-resolution thermal analysis shows the decomposition takes place in five steps. Each step is related to the loss of water, hydroxyl units, carbonate and sulphate. Infrared emission spectroscopy clearly identifies the presence of these molecular species and the temperature at which they are lost. Minor amounts of carbonate are observed in the minerals. Water is in two states in the structure, namely weakly hydrogen bonded and strongly hydrogen bonded. The symmetry of the sulphate anion is reduced through this hydrogen bonding.

© 2003 Elsevier Science B.V. All rights reserved.

**Keywords:** Dehydration; Dehydroxylation; Hydrotalcite; Infrared emission spectroscopy; High-resolution thermogravimetric analysis

## 1. Introduction

Interest in the study of hydrotalcites results from their potential use as catalysts [1–5]. The reason for the potential application of hydrotalcites as catalysts rests with the ability to make mixed metal oxides at the atomic level, rather than at a particle level. Such mixed metal oxides are formed through the thermal decomposition of the hydrotalcite [6,7]. Hydrotalcites may also be used as components in new nano-materials such as nano-composites [8]. There are many other

uses of hydrotalcites. Hydrotalcites are important in the removal of environmental hazards in acid mine drainage [9,10]. Hydrotalcite formation also offers a mechanism for the disposal of radioactive wastes [11]. Hydrotalcite formation may also serve as a means of heavy metal removal from heavy metal contaminated waters [12]. These hydrotalcites are readily synthesised by a co-precipitation method [13–15].

Hydrotalcites, or layered double hydroxides (LDH) are fundamentally anionic clays, and are less well known and more diffuse in nature than cationic clays like smectites [16,17]. The structure of hydrotalcite can be derived from a brucite structure ( $\text{Mg}(\text{OH})_2$ ) in which, e.g.  $\text{Al}^{3+}$  or  $\text{Fe}^{3+}$  (pyroaurite–sjögrenite)

\* Corresponding author.

E-mail address: [r.frost@qut.edu.au](mailto:r.frost@qut.edu.au) (R.L. Frost).

substitutes a part of the  $\text{Mg}^{2+}$ . This substitution creates a positive layer charge on the hydroxide layers, which is compensated by interlayer anions or anionic complexes [18,19]. In hydrotalcites a broad range of compositions are possible of the type  $[\text{M}_{1-x}^{2+}\text{M}_x^{3+}(\text{OH})_2][\text{A}^{n-}]_{x/n}\cdot y\text{H}_2\text{O}$ , where  $\text{M}^{2+}$  and  $\text{M}^{3+}$  are the di- and trivalent cations in the octahedral positions within the hydroxide layers with  $x$  normally between 0.17 and 0.33.  $\text{A}^{n-}$  is an exchangeable interlayer anion [20]. There exists in nature a significant number of hydrotalcites which are formed as deposits from ground water containing  $\text{Ni}^{2+}$  and  $\text{Fe}^{3+}$  [21]. These are based upon the dissolution of Ni–Fe sulphides during weathering. Among these naturally occurring hydrotalcites are carboydite and hydrohonessite [22,23]. These two hydrotalcites are based upon the incorporation of sulphate into the interlayer with expansions of 10.34–10.8 Å. Normally, the hydrotalcite structure based upon takovite (Ni, Al) and hydrotalcite (Mg, Al) has basal spacings of  $\sim 8.0$  Å where the interlayer anion is carbonate. If the carbonate is replaced by sulphate then the mineral carboydite is obtained. Similarly reevesite is the Ni, Fe hydrotalcite with carbonate as the interlayer anion, which when replaced by sulphate the minerals honessite and hydrohonessite are obtained.

The use of thermal analysis techniques for the study of the thermal decomposition of hydrotalcites is common [24]. Heating sjögrenite or pyroaurite at  $<200$  °C caused the reversible loss of  $\text{H}_2\text{O}$ . At 200–250 °C on static heating, or 200–350 °C on dynamic heating, very little  $\text{H}_2\text{O}$  or  $\text{CO}_2$  were lost, but changes in the infrared spectrum and DTA effects were observed [24]. To date the number of thermal analysis studies of these minerals is very limited. No studies of the thermal decomposition of carboydite and hydrohonessite have been forthcoming.

## 2. Experimental

### 2.1. Minerals

The minerals carboydite and hydrohonessite were obtained from CSIRO and originated from Western Australia [25,26]. The composition of the minerals was checked using an electron probe. The phase com-

position was determined by X-ray diffraction. Both minerals were found to be phase pure.

### 2.2. Thermal analysis

Thermal decomposition of the hydrotalcite was carried out in a TA<sup>®</sup> Instruments incorporated high-resolution thermogravimetric analysis (HRTG) (series Q500) in a flowing nitrogen atmosphere (80 cm<sup>3</sup>/min). Approximately 50 mg of sample was heated in an open platinum crucible at a rate of 2.0 °C/min up to 500 °C. With the quasi-isothermal, quasi-isobaric heating program of the instrument, the furnace temperature was regulated precisely to provide a uniform rate of decomposition in the main decomposition stage. The TGA instrument was coupled to a Balzers (Pfeiffer) mass spectrometer for gas analysis. Only selected gases were analysed.

### 2.3. Infrared emission spectroscopy

FTIR emission spectroscopy was carried out on a Nicolet spectrometer equipped with a TGS detector, which was modified by replacing the IR source with an emission cell. A description of the cell and principles of the emission experiment have been published elsewhere. Approximately 0.2 mg of the hydrotalcite mineral was spread as a thin layer (approximately 0.2 μm) on a 6 mm diameter platinum surface and held in an inert atmosphere within a nitrogen-purged cell during heating. Details of the technique have been published by the authors [27,28]. Spectral manipulation such as baseline adjustment, smoothing and normalisation was performed using the GRAMS<sup>®</sup> software package (Galactic Industries Corporation, Salem, NH, USA).

## 3. Results and discussion

### 3.1. High-resolution thermogravimetric analysis and mass spectrometric analysis

The HRTG of carboydite is shown in Fig. 1. Five principal weight loss steps are observed at 74, 99.6, 195, 407 and 703 °C. Thermal decomposition causes the loss of water initially. The initial weight loss including the steps at 74 and 99.6 °C is around 14%. Calculations for the weight loss based upon the

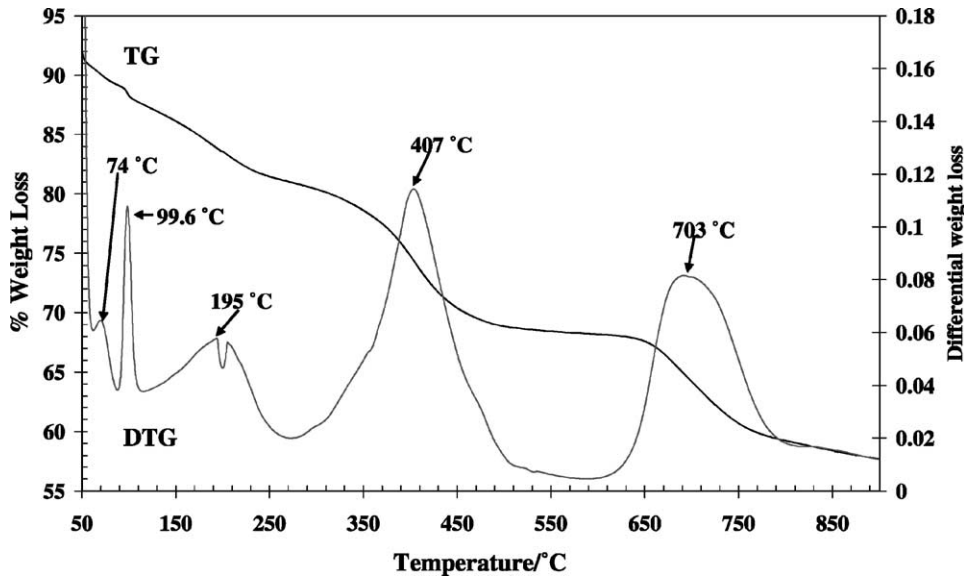


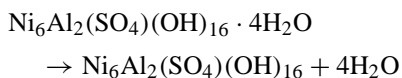
Fig. 1. TG and DTG curves for carboydite.

formula  $(\text{Ni}_6\text{Al}_2(\text{SO}_4)(\text{OH})_{16}\cdot 4\text{H}_2\text{O})$  is 14.0%. The broad weight loss step over the 100–250 °C is 6.5%. The weight loss step at 407 °C is 12.0%. These two steps are assigned to the dehydroxylation of the carboydite. The experimentally determined weight loss for the carboydite is 18.5% which may be compared with a theoretical weight loss of 35.1%. The final weight loss step is 11.6% and is attributed to sulphate loss as  $\text{SO}_2$ . The theoretical weight loss step is 12.4%.

The mass spectrometric analyses together with the DTGA patterns of carboydite are shown in Fig. 2. What may be clearly observed is that the first four weight loss steps can be attributed to water loss either through dehydration or dehydroxylation. The mass gain of  $\text{CO}_2$  is minimal for carboydite showing the mineral formulation as  $(\text{Ni}_6\text{Al}_2(\text{SO}_4)(\text{OH})_{16}\cdot 4\text{H}_2\text{O})$  is good. The mass loss step at 703 °C is assignable to the interlayer anion sulphate decomposition.

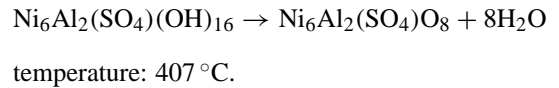
The following chemical reactions for the thermal decomposition of carboydite are proposed:

- Decomposition Steps 1 and 2

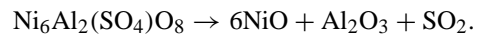


temperature: 95.6 °C.

- Decomposition Steps 3 and 4



- Decomposition Step 5



The TG and DTGA patterns for hydrohonessite are reported in Fig. 3. Hydrohonessite has a formula  $\text{Ni}_6\text{Fe}_2(\text{SO}_4,\text{CO}_3)(\text{OH})_{16}\cdot 7\text{H}_2\text{O}$ . The difference between hydrohonessite and honessite simply rests with the amount of hydration. Honessite has four molecules of water per formula unit and hydrohonessite approximately seven molecular units of water. Honessite is related to the mineral reevesite. The difference is simply the interlayer anion. In the case of honessite and hydrohonessite, it is the sulphate anion. In the example of reevesite it is carbonate. In some ways this imposes a difficulty for natural minerals in that mixed species can be obtained, i.e. both carbonate and sulphate exist in the interlayer. Thus, the natural mineral is some composition between the end members of reevesite and hydrohonessite.

Three weight loss steps are observed which are attributed to dehydration. These are observed at 71, 95.6

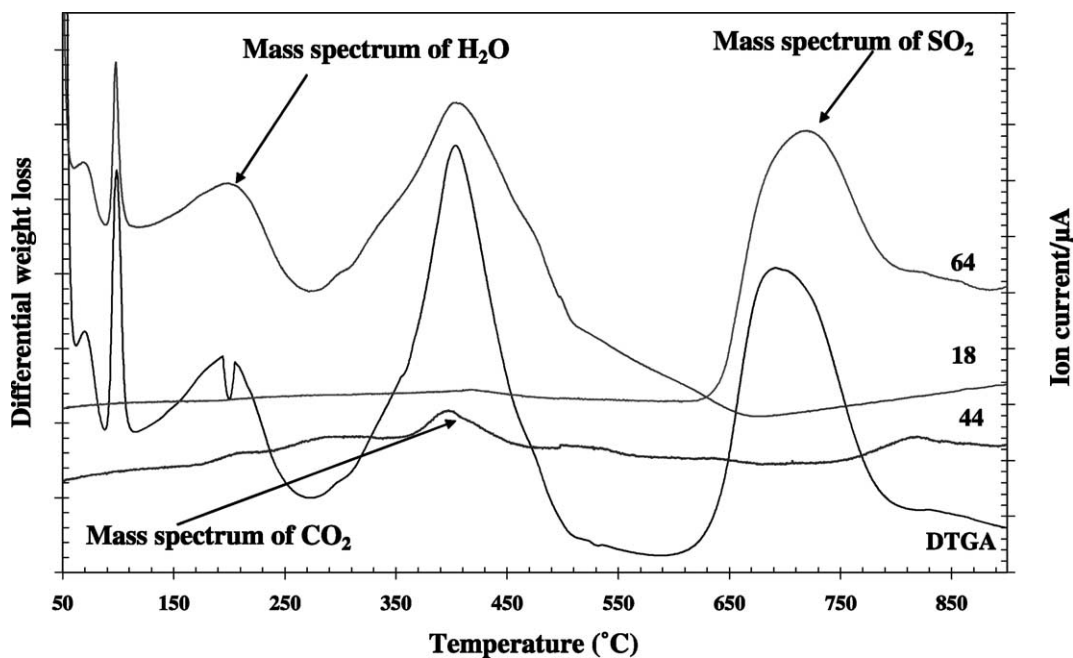


Fig. 2. MS and DTG curves for carbohydrite.

and 137 °C with weight losses of 2.3, 1.56 and 5.2%. The total weight loss ascribed to dehydration is 9.06%. Based on the formula  $\text{Ni}_6\text{Fe}_2(\text{SO}_4)(\text{OH})_{16}\cdot 7\text{H}_2\text{O}$  the theoretical weight loss for dehydration is 13.15%

based upon seven molecules of water in the formula. If there are four water molecules in the formula unit then the theoretical weight loss of 7.9% is obtained. Thus, the experimental result for dehydration is between

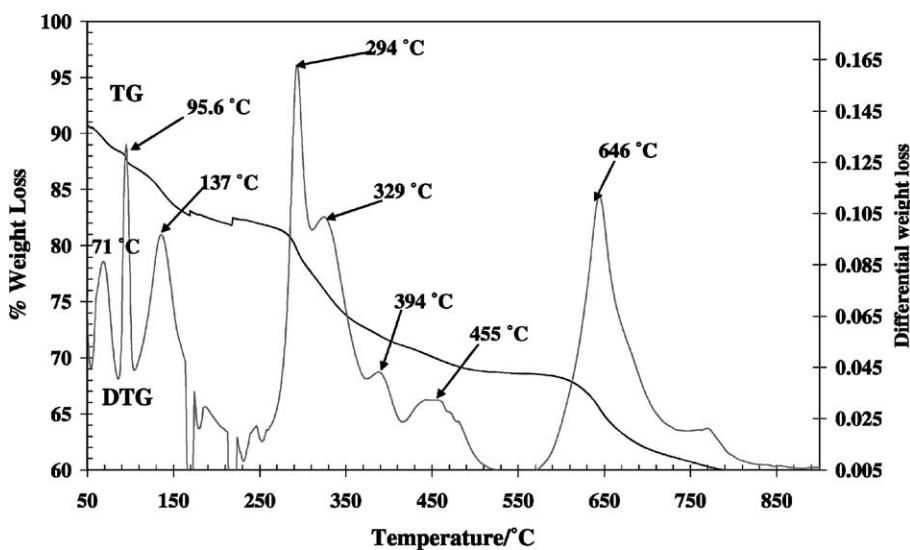


Fig. 3. TG and DTG curves for hydrohonessite.

that of honessite and hydrohonessite. Such a result is not unexpected as these minerals may dehydrate and rehydrate quite readily. Two weight loss steps are observed at 294 and 329 °C with a total weight loss of 10.5%. These two steps are attributed to dehydroxylation. The theoretical weight loss for dehydroxylation is 28.39% based upon the hydrohonessite formula. There is an apparent large difference between the experimentally determined and theoretical calculated results. This means that the number of hydroxyl units in the formula is not 16 but some number less. Two further weight loss steps are observed at 394 and 455 °C. The total for these two steps is 4.0%. This weight loss step is attributed to the loss of carbonate. The final weight loss step is observed at 646 °C, and is attributed to loss of sulphate.

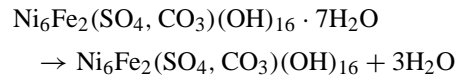
The complexity of the DTGA patterns is reflected in the mass spectrum of hydrohonessite. The mass spectrometric analyses together with the DTGA patterns of hydrohonessite are shown in Fig. 4. The difference between the MS patterns of carboydite and hydrohonessite are summarised as follows:

(a) The hydrohonessite has significantly more carbonate in the structure.

- (b) More steps are involved in the thermal decomposition of hydrohonessite.
- (c) In general, the temperature of decomposition for each step is less for hydrohonessite than that for carboydite.

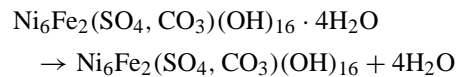
The following mechanisms are suggested for the thermal decomposition of hydrohonessite:

- Decomposition Step 1



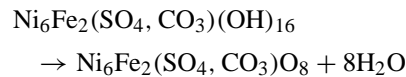
temperature: 95.6 °C.

- Decomposition Step 2



temperature: 137 °C.

- Decomposition Steps 3 and 4



temperatures: 294 and 329 °C.

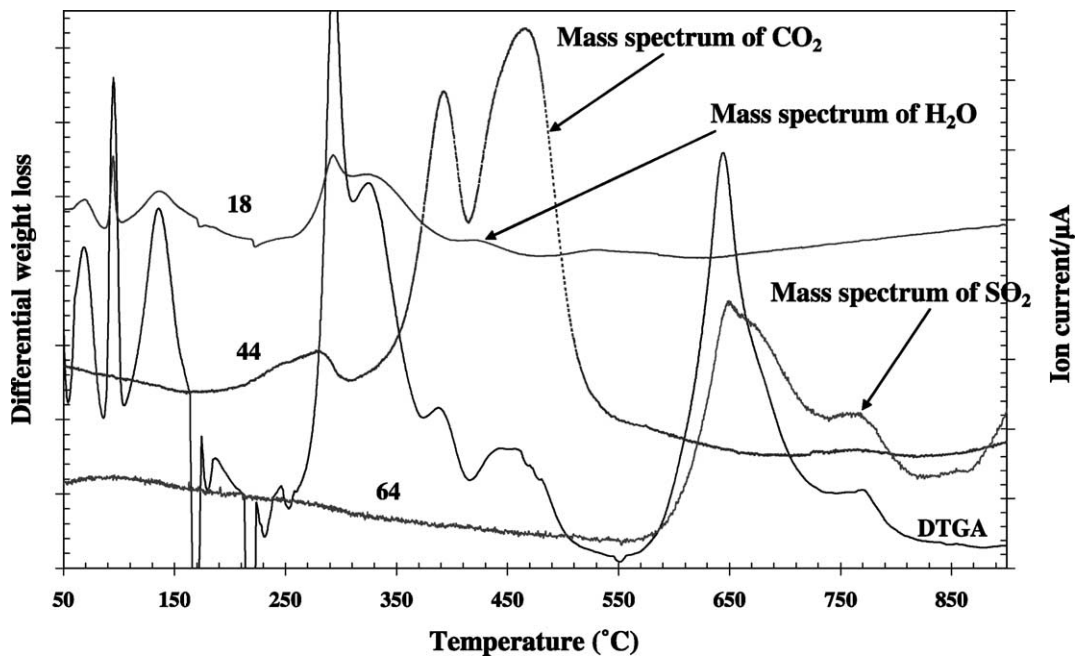


Fig. 4. MS and DTG curves for hydrohonessite.

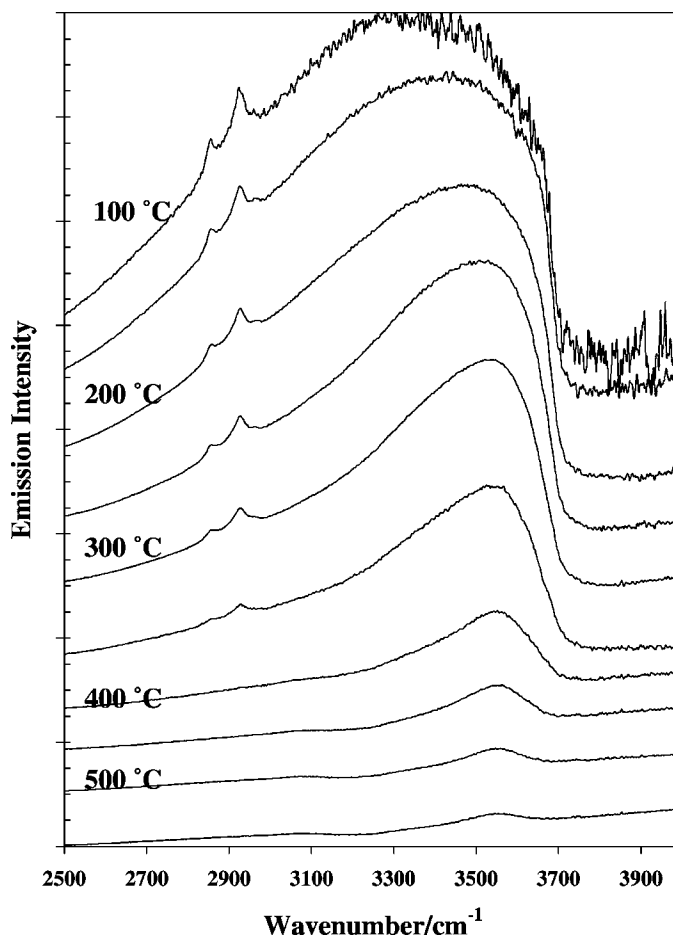
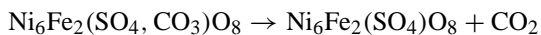


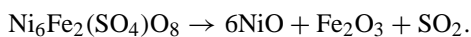
Fig. 5. Infrared emission spectra of the hydroxyl stretching region of carboydite.

- Decomposition Step 5



temperatures: 394 and 455 °C.

- Decomposition Step 6



### 3.2. Infrared emission spectroscopy of carboydite and hydrohonessite

One method of following the thermal decomposition of these natural hydrotalcites is to use a combination of vibrational spectroscopy and a thermal stage. Infrared emission spectroscopy is one of these tech-

niques [29–32]. The infrared emission spectra of carboydite are shown in Fig. 5. The spectra at the lower temperatures appear with low signal to noise. This is because of the low energy of thermal emission at the lower temperatures, namely 50, 75 and 100 °C. As the temperature is raised the energy of emitted radiation is increased and the signal to noise ratio improves. The spectra in the hydroxyl stretching region are then band fitted to find the position and relative intensity of the bands.

In the 100 °C spectrum, three overlapping bands are observed at 3040, 3372 and 3578  $\text{cm}^{-1}$ . The first two bands are assigned to the OH stretching modes of water and the last band to the OH stretching vibration of the hydroxyl units in the carboydite structure. The intensity of the first two bands approaches

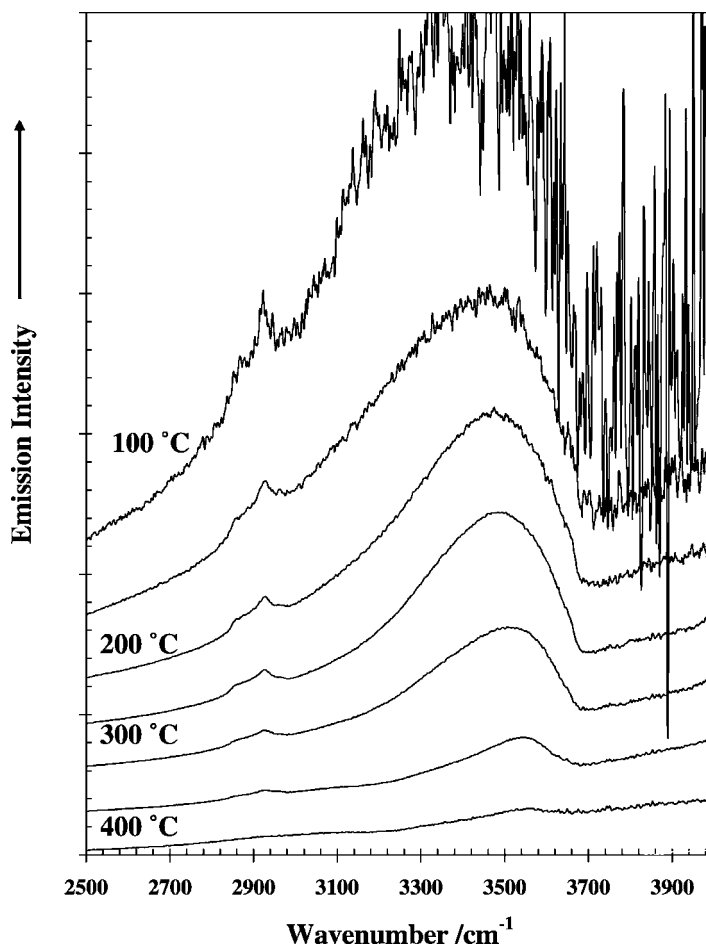


Fig. 6. Infrared emission spectra of the hydroxyl stretching region of hydrohonesite.

zero by 400 °C and intensity remains in the hydroxyl stretching vibration of the OH units up to 500 °C. These bands show a red shift with heating. The bands are observed at 3090, 3411 and 3588  $\text{cm}^{-1}$  at 250 °C. At 350 °C, the bands are observed at 3370, 3542 and 3617  $\text{cm}^{-1}$ . The infrared emission spectra of the hydroxyl stretching region of hydrohonesite are shown in Fig. 6. The intensity of the hydroxyl stretching region is lost by 400 °C. The temperatures for the dehydroxylation are in harmony with the TG results. The thermal decomposition of hydrohonesite takes place at lower temperatures than carboydite.

In the infrared emission spectrum of hydrohonesite at 150 °C, three overlapping bands are observed at 3101, 3371 and 3540  $\text{cm}^{-1}$ . The first two bands are

assigned to the hydroxyl stretching vibrations of water and the band at 3540  $\text{cm}^{-1}$  to the OH stretching vibration of the OH units. In the 250 °C, spectrum these bands are observed at 3406, 3521 and 3604  $\text{cm}^{-1}$ .

The infrared emission spectra of carboydite in the  $\text{SO}_4$  and  $\text{CO}_3$  stretching region are shown in Fig. 7. The spectra show the thermal decomposition steps in line with the chemical reactions proposed above. The spectrum is most interesting as it shows the features that are observed in the HRTG and MS patterns. The spectrum shows three bands at 1054, 1107 and 1159  $\text{cm}^{-1}$ , attributed to the  $\text{SO}_4$  antisymmetric stretching vibrations. There is a small inflection in the spectrum at 973  $\text{cm}^{-1}$  which is assigned to the  $\text{SO}_4$  symmetric stretching vibration. The observation

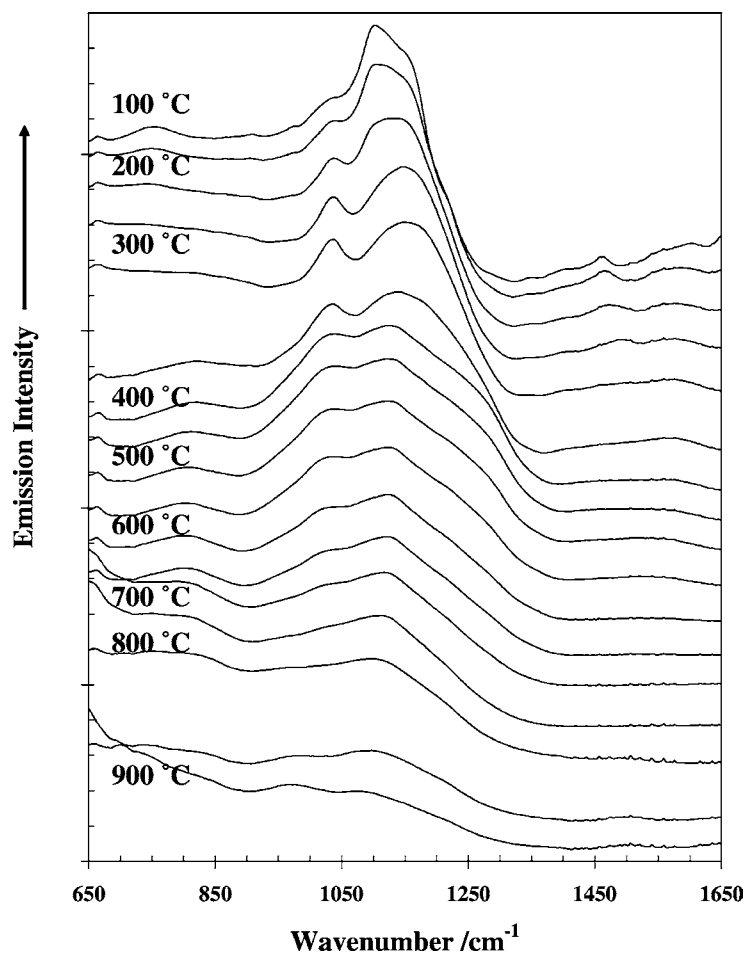


Fig. 7. Infrared emission spectra of the  $\text{SO}_4$  stretching region of carboydite.

of multiple antisymmetric stretching vibrations shows the reduction in symmetry of the sulphate anion in the interlayer. It is suggested that this reduction in symmetry is brought about through hydrogen bonding to both the water molecules in the interlayer and to the surface hydroxyls. Two other bands of significantly lower intensity are observed at  $1405$  and  $1459\text{ cm}^{-1}$ . These bands are assigned to the  $\text{CO}_3$  antisymmetric stretching vibrations. The observation of carbonate even though of very low concentrations is in harmony with the MS results where some very minor evolved  $\text{CO}_2$  gas was observed. The spectra also show two bands at  $1612$  and  $1670\text{ cm}^{-1}$ . These two bands are assigned to the bending modes of water. The fact that two bands are observed with different

wavenumbers rests with the differences in hydrogen bonding strength. The band at  $1670\text{ cm}^{-1}$  is attributed to water which is strongly hydrogen bonded to the hydroxyl units of Ni and Al. An alternative explanation is that the water is strongly hydrogen bonded to the sulphate anions. This explanation appears less likely. The  $1612\text{ cm}^{-1}$  band is assigned to weakly hydrogen bonded water. Such water fills the interlayer and could be scribed to water bonding to other water molecules.

The set of spectra clearly show the phase changes involved in the thermal decomposition of this mineral. As for the analysis of the IE spectra of carboydite, three sets of bands are observed. Firstly, the bands observed at  $978$ ,  $1049$  and  $1151\text{ cm}^{-1}$  are assigned



to the  $\text{SO}_4$  symmetric and antisymmetric stretching vibrations. Secondly, a complex band profile is centred on  $1446\text{ cm}^{-1}$  ascribed to the  $\text{CO}_3$  antisymmetric stretching vibrations. Thirdly, the bands observed at  $1614$  and  $1654\text{ cm}^{-1}$  are assigned to the water bending modes. In the IE spectrum at  $200^\circ\text{C}$ , bands are observed at  $1030$ ,  $1096$  and  $1159\text{ cm}^{-1}$ . These bands are assigned to the  $\text{SO}_4$  antisymmetric stretching modes. The broad profile at  $1441\text{ cm}^{-1}$  is attributed to the antisymmetric  $\text{CO}_3$  stretching modes. What is noted is the absence of any HOH bending modes. At this temperature no water is observed in the IE spectra. The spectrum at  $600^\circ\text{C}$  shows the absence of both water and carbon dioxide. At this temperature the  $\text{SO}_4$  spectra become less complex. Only two bands are observed at  $972$  and  $1121\text{ cm}^{-1}$  assigned to the  $\text{SO}_4$  symmetric and antisymmetric stretching modes. The reason why the spectra have become simple is due to the lack of either water or OH units with which the sulphate could hydrogen bond.

#### 4. Conclusions

The HRTGA of the two related minerals carboydite and hydrohonesite have been studied. These hydroalcalite minerals show at least five weight loss steps ascribed to (a) water desorption, (b) dehydration, (c) dehydroxylation, (d) de-carbonate-ing (hydrohonesite), and (e) de-sulphating.

The differences in the thermal decomposition between the two minerals are:

- (a) The hydrohonesite has significantly more carbonate in the structure.
- (b) More steps are involved in the thermal decomposition of hydrohonesite.
- (c) In general, the temperature of decomposition for each step is less for hydrohonesite than that for carboydite.

The thermal analysis results are complemented by the infrared emission spectra. These spectra confirm the presence of carbonate in both minerals but only in very low concentrations. This suggests that the formula of carboydite and hydrohonesite as written is correct, namely  $\text{Ni}_6\text{Al}_2(\text{SO}_4,\text{CO}_3)(\text{OH})_{16}\cdot 4\text{H}_2\text{O}$  and  $\text{Ni}_6\text{Fe}_2(\text{SO}_4,\text{CO}_3)(\text{OH})_{16}\cdot 7\text{H}_2\text{O}$ , respectively. The IE spectra show the temperatures at which the water, the

hydroxyls and the carbonate is lost. The sulphate is lost at significantly higher temperatures.

#### References

- [1] J.T. Klopogge, R.L. Frost, *Appl. Catal. A: Gen.* 184 (1999) 61.
- [2] A. Alejandre, F. Medina, X. Rodriguez, P. Salagre, Y. Cesteros, J.E. Sueiras, *Appl. Catal. B* 30 (2001) 195.
- [3] J. Das, K. Parida, *React. Kinet. Catal. Lett.* 69 (2000) 223.
- [4] S.H. Patel, M. Xanthos, J. Greci, P.B. Klepak, *J. Vinyl Addit. Technol.* 1 (1995) 201.
- [5] V. Rives, F.M. Labajos, R. Trujillano, E. Romeo, C. Royo, A. Monzon, *Appl. Clay Sci.* 13 (1998) 363.
- [6] F. Rey, V. Fornes, J.M. Rojo, *J. Chem. Soc., Faraday Trans.* 88 (1992) 2233.
- [7] M. Valcheva-Traykova, N. Davidova, A. Weiss, *J. Mater. Sci.* 28 (1993) 2157.
- [8] C.O. Oriakhi, I.V. Farr, M.M. Lerner, *Clays Clay Miner.* 45 (1997) 194.
- [9] G. Lichti, J. Mulcahy, *Chem. Aust.* 65 (1998) 10.
- [10] Y. Seida, Y. Nakano, *J. Chem. Eng. Jpn.* 34 (2001) 906.
- [11] Y. Roh, S.Y. Lee, M.P. Elless, J.E. Foss, *Clays Clay Miner.* 48 (2000) 266.
- [12] Y. Seida, Y. Nakano, Y. Nakamura, *Water Res.* 35 (2001) 2341.
- [13] M.A. Aramendia, V. Borau, C. Jimenez, J.M. Marinas, J.M. Luque, J.R. Ruiz, F.J. Urbano, *Mater. Lett.* 43 (2000) 118.
- [14] V.R.L. Constantino, T.J. Pinnavaia, *Inorg. Chem.* 34 (1995) 883.
- [15] M. Del Arco, P. Malet, R. Trujillano, V. Rives, *Chem. Mater.* 11 (1999) 624.
- [16] K. Hashi, S. Kikkawa, M. Koizumi, *Clays Clay Miner.* 31 (1983) 152.
- [17] L. Ingram, H.F.W. Taylor, *Mineral. Mag. J. Mineral. Soc.* (1876–1968) 36 (1967) 465.
- [18] R.M. Taylor, *Clay Miner.* 17 (1982) 369.
- [19] H.F.W. Taylor, *Mineral. Mag. J. Mineral. Soc.* (1876–1968) 37 (1969) 338.
- [20] H.C.B. Hansen, C.B. Koch, *Appl. Clay Sci.* 10 (1995) 5.
- [21] E.H. Nickel, J.E. Wildman, *Mineral. Mag.* 44 (1981) 333.
- [22] D.L. Bish, A. Livingstone, *Mineral. Mag.* 44 (1981) 339.
- [23] E.H. Nickel, R.M. Clarke, *Am. Mineral.* 61 (1976) 366.
- [24] P.G. Rouxhet, H.F.W. Taylor, *Chimia* 23 (1969) 480.
- [25] E.H. Nickel, R.M. Clarke, *Am. Miner.* 61 (1976) 366.
- [26] E.H. Nickel, J.E. Wildman, *Miner. Mag.* 44 (1981) 333.
- [27] R.L. Frost, A.M. Vassallo, *Clays Clay Miner.* 44 (1996) 635.
- [28] R.L. Frost, B.M. Collins, K. Finnie, A.J. Vassallo, *Clays controlling environment*, in: *Proceedings of the 10th International Clay Conference*, Adelaide, 18–23 July 1993, 1995, p. 219.
- [29] R.L. Frost, G.A. Cash, J.T. Klopogge, *Vib. Spectrosc.* 16 (1998) 173.
- [30] J.T. Klopogge, S. Komarneni, K. Yanagisawa, R. Fry, R.L. Frost, *J. Colloid Interface Sci.* 212 (1999) 562.
- [31] J.T. Klopogge, R. Fry, R.L. Frost, *J. Catal.* 184 (1999) 157.
- [32] J.T. Klopogge, R.L. Frost, *An infrared emission spectroscopic study of synthetic and natural pyrophyllite*. *Neues Jahrbuch fuer Mineralogie, Monatshefte* (1999) (2), 62–74.